Answers to reviewer 1 (Paper-IOP16-NHESS)

We would like to thank the anonymous reviewer for the valuable comments, suggestions and questions. We have considered all comments. We believe that the quality of the manuscript has increased, thanks to the comments of the reviewer and acknowledge how answering the raised questions has been crucial for a better exposition of our key messages.

1 - GENERAL COMMENTS

R1C1. First of all, it contains numerous purely speculative assertions that are not at all substantiated. This is reinforced by the fact that results are often given before they are demonstrated (this should be reversed). More rigorous justifications are needed to make the discussion paper a compelling study.

We have corrected all speculative answers and hypothesis in the manuscript, as well as reorganized the conclusions to be given after presenting the corresponding results only.

We would like to add, that this case study belongs to a series of modelling experiments performed in our group which are object of an on-going publication. In these modelling experiments we analysed the impact of nudging GPS-ZTD on several heavy precipitation events of the HyMeX period as well as the statistics of the complete autumn season. This is why at times in the manuscript some statements are introduced which are not justified. These statements arise from further analysis on the period which are not presented in the paper. This has been corrected accordingly to show only information relative to IOP16.

R1C2. Second, as justly stated by the authors at the end of their concluding section, their study relies on one case only. This undermines the results concerning the sensitivity study to the assimilation of GPS ZTD data

We have adapted the manuscript to clearly state that the withdrawn conclusions correspond to the presented case only (IOP16). This is done for example at lines L579-580.

In connection with the previous answer, we will submit in the coming weeks a publication with analyses on heavy precipitation and the impact of the GPS-ZTD nudging for the whole season. The selected case study object of this paper is a relevant event of the period since the GPS-ZTD showed very interesting impacts on convective development, as explained in the manuscript. The simulations presented in this paper are used, together with other simulations and observational data, in the analyses of this future publication on the seasonal time scale.

To let the readers know about the broader scope of these studies we have adapted the following section.

2.2.2 The GPS-ZTD Nudging Sensitivity Experiments (L244-246)

IOP16, the case study of this paper, is one of them which is especially interesting given the large reduction of maximum precipitation (-20 %) induced by the GPS-ZTD nudging over the investigation area of Corsica in the course of 26 h. The remaining cases of the autumn 2012 period and analyses on the complete season are part of a series of modelling studies from our working group, including a PhD thesis by Caldas-Alvarez (2019). IOP16 is also suitable to assess the benefit of atmospheric moisture corrections with GPS-ZTD nudging given the important role of the local orographic and instability factors in triggering and maintaining convection rather than the large-scale upper level forcing.

R1C3. all the more since the different runs start much earlier than the event itself. In doing so, it is difficult to link the impact of the assimilation of ZTD-GPS data to the simulated precipitation. Differences observed during the chosen event might simply be due to the chaotic nature of the atmosphere. In any case, such a configuration does

This is in connection with the previous answers. We believe that analysing one case study from a seasonal simulation can be useful to relate the findings for this one case study with the analysis of the whole Autumn period. In addition, we think that starting the simulation 50 days before the event allows us to study the hypothesis that correcting the atmospheric moisture also during previous events (not only during the selected case study) would bring a larger improvement for precipitation. In this sense we wanted to profit from the availability of the unique GPS-ZTD data set, that covers the whole SOP1 period and part of 2013 (1-Sep-2012 to 20-Nov-2013). Moreover, the earlier initialization introduces a spin up time for slower processes such as soil-atmosphere interactions that are affected by precipitation during previous events.

Since we consider relevant the question raised by the reviewer, how different the impact will be depending on the initialization day, we performed additional simulations starting only a few days before the event using the same settings and forcing data but initialized on the 20-Oct-2012. This date was selected to ensure the representation of the large moisture evapotranspiration over north Africa (20 to 21-Oct), demonstrated in Fig. 6 of the manuscript.
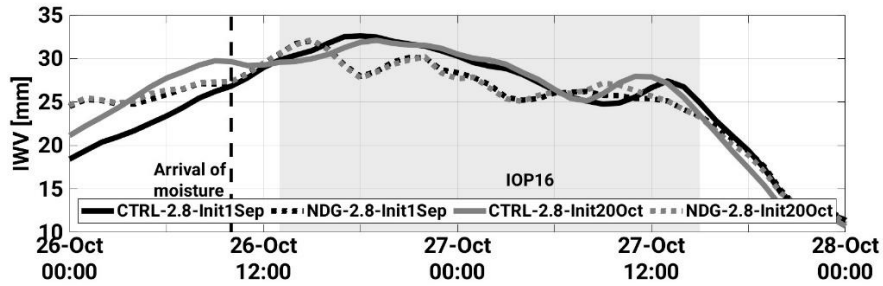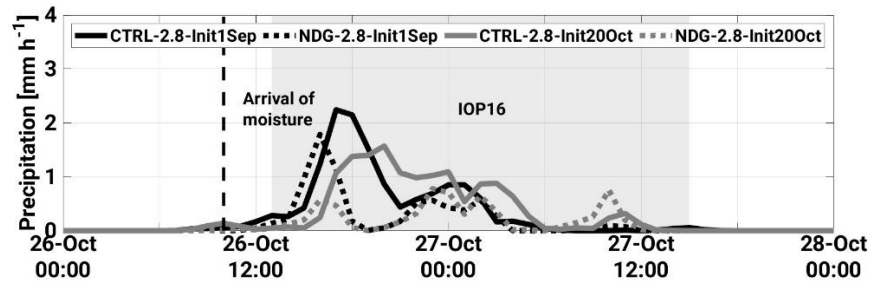
a)
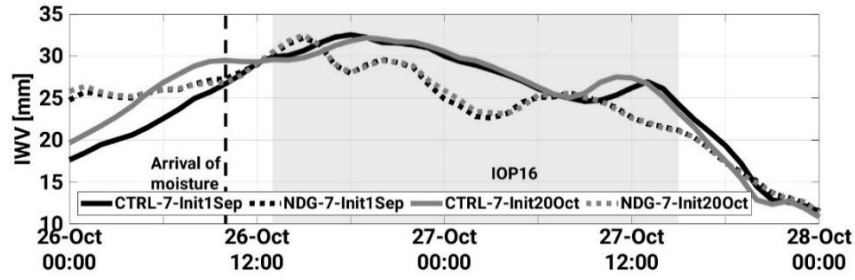
b)
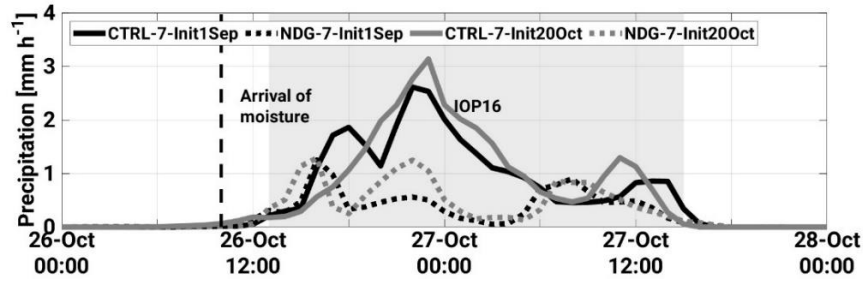
c)

d)

Figure 1. Spatially averaged IWV (a, c) and Precipitation (b, d) for the 7 km simulations (a, b) and the 2.8 km (c, d) during the event. The area of the spatial averages is Corsica. The model output has been upscaled to a common coarser grid of 8 km to allow for comparison. The period shown is 26-Oct 0000 UTC to 28-Oct 0000 UTC.

Regarding IWV, the shorter simulations show differences in that the IWV increase happens 1 to 2 h earlier in the CTRL runs initialized on the 20-Oct (Init20Oct). This holds for both resolutions. The NDG runs show, however, no perceptible differences for the temporal evolution of spatially averaged hourly IWV. On the contrary, precipitation shows relevant differences for both resolutions (Fig. 1b and Fig.1.d). NDG-7-Init20ct shows two maxima instead of three with somewhat larger precipitation intensities. NDG-2.8-Init20Oct shows a delayed (1 h) onset of precipitation and lower precipitation rates as compared to CTRL-2.8-Init1Sep.

A plausible explanation for these findings, as stated by the reviewer, is the chaotic nature of the atmosphere that is affected by all perturbations in earlier stages. This analysis will be added in the annex of the manuscript as supplementary information for the readers. We prefer not to include it in the body of the paper, since it deviates from the objective for the article.

We believe using the longer simulations, i.e. started on the 1-Sep-2012, have the advantage of relating the findings with those of our planed publication on the complete autumn season and that they benefit from the whole duration of the GPS-ZTD data set. Therefore, we will present in our manuscript the analyse with these simulations as in the first version but will add a supplementary subsection within *4-Nudging Effects on Convection* where the sorter simulations will be introduced and analysed. This will be done to present the results of the 1h vs. 10min frequency comparison (see comment R1C5).

R1C4. authors should include some estimation of the impact duration of the GPS-ZTD data assimilation by running some free runs and determining when they converge

Our simulations span the whole autumn season to cover the duration of the HyMeX SOP1 and the availability of the GPS-ZTD data. This is why it is not possible to answer when would the assimilated and the free runs converge. Our scientific question was *how is convective precipitation impacted by a continuous correction of IWV in the model?* The modelling set up was planned in a different way to usual data-denial assimilation experiments (Borderies, et al., 2019; Benjamin, et al., 2010; Mahfouf, et al., 2015) in that these experiments data assimilation is performed during a given time window to obtain the initial conditions for a future step of first guesses. These data-denial experiments allow to study how long the impact of an observation type stays in the system as the analysed runs converge with the forecasts, but our set-up was not conceived to provide information on this.

R1C5. the benefit of a sub-hourly frequency versus, e.g., at hourly frequency, has not been demonstrated (coming from my sentence "modelling experiments demonstrated the benefit of sub-hourly GPS-ZTD nudging to improve the modelling of precipitation")

Thanks for this comment. We acknowledge that the sentence was misleading. We wanted to express that our experiments nudging GPS-ZTD with a 10-min frequency showed an improvement for this case study. This has been corrected in the manuscript.

We agree that this is an interesting aspect, thus we have performed supplementary simulations to investigate more in detail this issue. We run the 20-Oct-2012 to 28-Oct-2012 0000 UTC period as in the comment R1C3, applying the GPS-ZTD nudging with a frequency of 1 h, as opposite to the 10 min frequency. All other settings are the same as NDG-7-Init20Oct and NDG-2.8-Init20Oct respectively. Hereafter we name these simulations simply as CTRL-7, CTRL-2.8, NDG-7, NDG-2.8, NDG-7-1h and NDG-2.8-1h. These six simulations have been initialized on the 20-Oct-2012
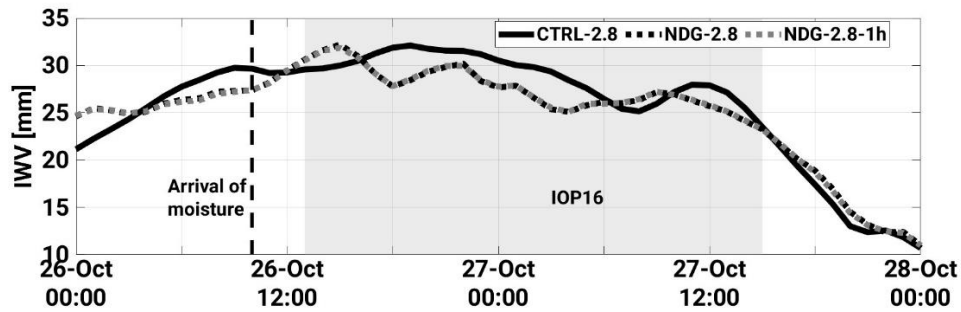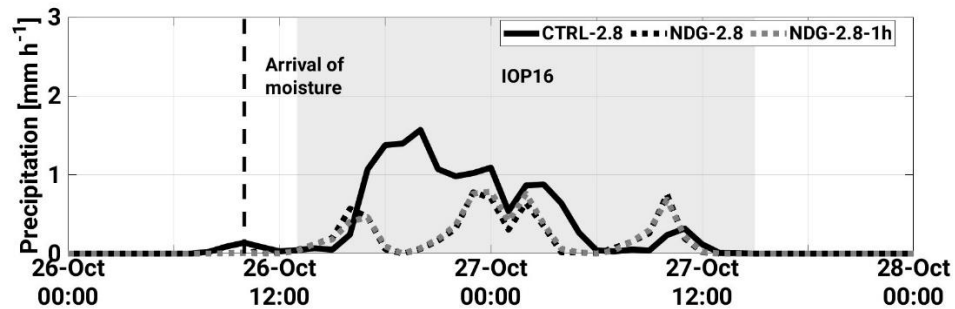
a)
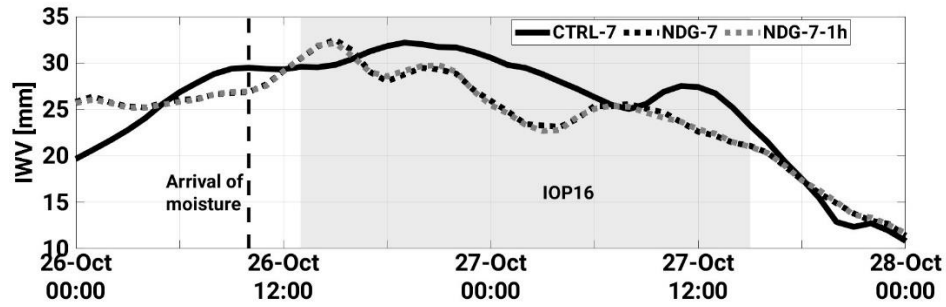
b)
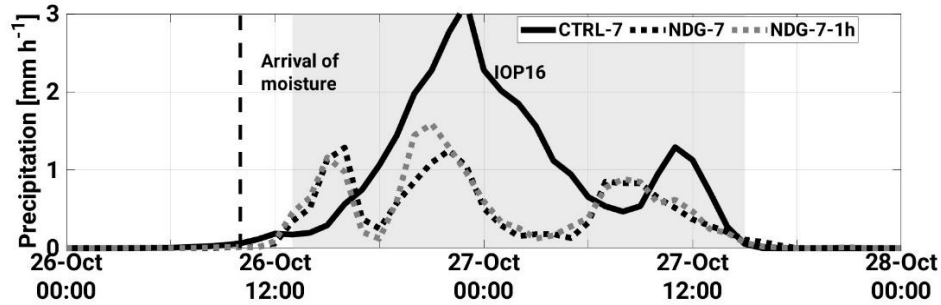
c)

d)

Figure 2. Spatially averaged IWV (a, c) and Precipitation (b, d) for the 7 km simulations (a, b) and the 2.8 km simulations (c, d) during the event. The area for averaging is Corsica. The model output has been upscaled to a common coarser grid of 8 km. The period shown is 26-Oct 0000 UTC to 28-Oct 0000 UTC. The comparison is between the runs using a temporal nudging frequency of 10 min (NDG-7, NDG-2.8) against nudging at a temporal frequency of 1h (NDG-7-1h, NDG-2.8-1h).

The results show no differences on the temporal evolution of IWV. This holds for 7 km and 2.8 km. This can be explained by the fact that we calculate the spatially averaged IWV at sharp hours (i.e. 0000 UTC, 0100 UUTC, 0200 UTC, etc.), precisely is at those times when the GPS-ZTD data is assimilated in the NDG-7-1h and the NDG-2.8-1h runs.

For precipitation, there is a slight impact for the 7 km runs, but not for the 2.8 km. The NDG-7-1h simulation shows a somewhat larger precipitation than NDG-7 at 2000 UTC on the 26-Oct (Fig. 2b) corresponding to an increase from 30 mm to 50 mm at the western shore of the island (Fig.3.b and Fig. 3.c).
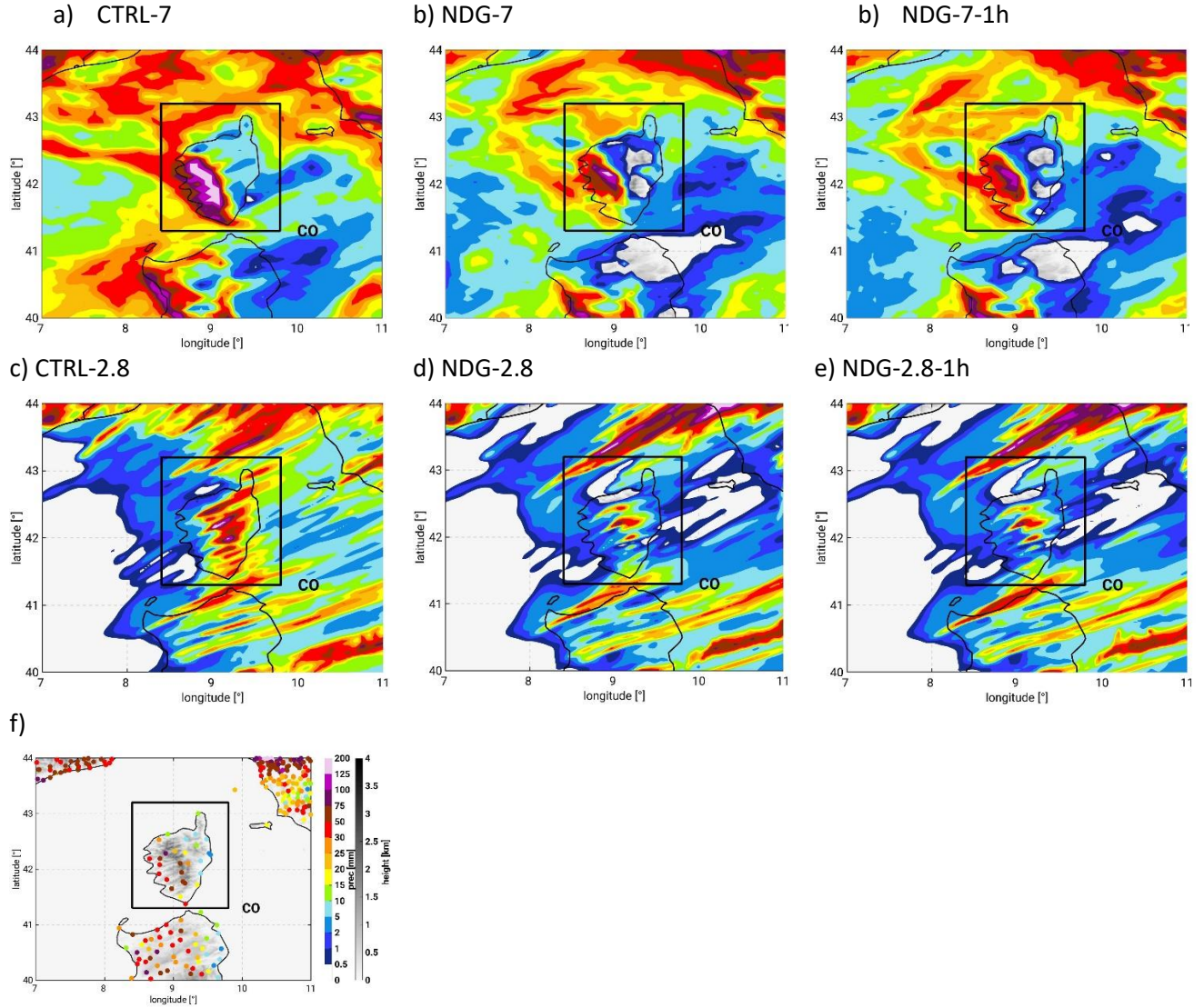
Figure 3. COSMO-CLM accumulated precipitation over Corsica between 26-Oct 1300 UTC and 27-Oct 1500 UTC i.e. during the period of precipitation over the island and RG.

To delve further into which aspects of precipitation representation have been improved, we present in Table 1 further validation metrics using the Rain Gauges (RG) as reference.

Table 1 shows the RMSE of the anomalies of hourly precipitation rates (first column), the differences (OBS-MOD) of the standard deviations of hourly precipitation (second column) and the spatially averaged differences of accumulated precipitation during the whole event, i.e. between 26-Oct 1300 UTC and 27-Oct 1500 UTC (third column). The last three metrics are obtained after interpolating the COSMO-CLM precipitation values to the location of the RG stations. On the other hand, columns four and five of Table 1, show differences of the standard deviation and maximum value of precipitation for COSMO-CLM over land without interpolation. That means, we have obtained all 27h-accumualeted precipitation values simulated by COSMO-CLM over land and have calculated the standard deviation and the maximum. We have done the same for all RG measurements and the

differences are shown. We do this to avoid double-penalty problems due to a possible misrepresentation of the maxima location (Wernli, et al., 2008; Gilleland, et al., 2009). The formulas used are included in Table 2.

Table 1. Metrics of the precipitation validation against RG. The model precipitation has been interpolated to the location of the RG for the first three columns and all precipitation values simulated by COSMO-CLM over the island of Corsica are used in the last two columns. This is done to avoid double-penalty problems due to a shifting of the precipitation maxima. N is the number of RG stations and M the total number of grid points over land. The units are mm.

[mm]		Interp. To RG location		Distributions without interpolation	
	RMSE (h)	$OBS_\sigma - MOD_\sigma$ (1h)	$\overline{OBS} - \overline{MOD}$ (27h)	$OBS_\sigma - MOD_\sigma$ (27h)	$OBS_{max} - MOD_{max}$ (27h)
CTRL-7-Init20Oct	3.3	-0.85	-19.1	-33	-170
NDG-7-Init20Oct	2.5	0.73	12.5	-5	-79
NDG-7-1h- Init20Oct	2.5	0.95	12.2	-4	-50
CTRL-2.8-Init20Oct	3.6	-0.15	9.5	-3	-74
NDG-2.8-Init20Oct	2.6	1.64	23.8	11	-16
NDG-2.8-1h- Init20Oct	2.5	1.64	23.6	10	-17

Table 2. Precipitation validation metrics.

RMSE (1h)	$\sqrt{\sum_{i(1h)}^{N} ((OBS_i - \overline{OBS}) - (MOD_i - \overline{MOD}))^2}$
$\boldsymbol{OBS_\sigma - MOD_\sigma}$ (1h)	$\sqrt{\frac{1}{N}\sum_{i(1h)}^{N} (OBS_i - \overline{OBS})^2} - \sqrt{\frac{1}{N}\sum_{i(1h)}^{N} (MOD_i - \overline{MOD})^2}$
$\boldsymbol{\overline{OBS} - \overline{MOD}}$ (27h)	$\frac{1}{N}\sum_{i(27h)}^{N} OBS_i - \frac{1}{N}\sum_{i(27h)}^{N} MOD_i$
$\boldsymbol{OBS_\sigma - MOD_\sigma}$ (27h)	$\sqrt{\frac{1}{N}\sum_{i(27h)}^{N} (OBS_i - \overline{OBS})^2} - \sqrt{\frac{1}{M}\sum_{j(27h)}^{M} \left(MOD_j - \overline{MOD}\right)^2}$
$\boldsymbol{OBS_{max} - MOD_{max}}$ (27h)	$\max(OBS_i) - \max(MOD_j)$

Overall, we see that nudging GPS-ZTD data is beneficial for the 7 km grid with little difference between nudging with 1h frequency or 10 min. If any, we see a slight advantage in nudging GPS-ZTD data with 10 min for the representation of the hourly standard deviation rates. The same holds for the 2.8 km, assimilating with a 10min frequency shows very weak differences with respect to assimilating with 1h frequency.

These results will be included as an additional subsection in section 4.1 (Nudging effects on Precipitation).

R1C5. there is no "pure" modelling in the study since the model is constantly perturbed by the modification of its moisture field. The authors should be more specific about the usefulness of continuously nudging moisture.

We decided to perform a continuous nudging to study the scientific question "how does simulated precipitating convection respond to a sub-hourly moisture correction?". In the following version of the manuscript we state more clearly that our study is diagnostic and that we do not provide an assessment of the prognostic use of GPS-ZTD nudging. We have corrected the following parts.

In the Abstract

"In this study, we use a diagnostic approach to assess the sensitivity of precipitating convection and underlying mechanisms during a heavy precipitation event (HyMeX intensive observation period 16) to corrections of the atmospheric moisture spatio-temporal distribution."

In Section 2.2.2 of the Methods. The GPS-ZTD Nudging Sensitivity Experiments

"The Nudging scheme is used to assimilate GPS-ZTD data to assess the sensitivity of heavy precipitating convection to corrections of the spatio-temporal distribution of atmospheric moisture. We use a diagnostic approach as opposite to commonly use data-denial experiments."

As stated earlier in this document, our modelling setup differs from other data-denial assimilation experiments for instance (Benjamin, et al., 2010; Borderies, et al., 2019; Sahlaoui, et al., 2019). Hence the idea of finding new initial conditions for subsequent forecast intervals through data assimilation does not apply in our experiments.

We believe, our study is valuable we were able to show the potential of such observation nudging since, for this case study, hourly RMSE values, the maximum and standard deviation were improved using the GPS-ZTD nudging and in the 7 km grid. Furthermore, we also observed the problems of COSMO in representing the moisture vertical gradient with substantial differences between 7 km and 2.8 km and how the GPS nudging could not correct sufficiently the vertical humidity errors. We saw that for this case study, the reduction of instability and of humidity at the free-troposphere exerted the largest control for convective precipitation. The fact that we nudge our simulations to GPS values continuously for a whole season has the advantage that the corrections introduced are not only present during the event (as usually in data-denial experiments) but also in past events.

2 - SPECIFIC COMMENTS

R1C6. L47-49: The authors point out the interest of assimilating humidity data at sub-hourly frequencies. I suggest the authors study the sensitivity of the assimilation frequency by carrying out an additional experiment with a one-hour assimilation frequency. This would demonstrate to what extent a sub-hourly assimilation frequency is needed.

See section 1.

R1C7. Case study and numerical set-up: Why run experiments that last several months and study one case only? The differences seen in this specific case could be caused by a lower predictability rather than to improvements in the description of the humidity field.

See section 1.

We decided to force the NDG-2.8 simulations with the CTRL-7 simulations to be able to compare NDG-2.8 to CTRL-2.8 directly. By doing so we were able to assess the direct impact of the GPS-ZTD nudging at the 2.8 km resolution which would have not been possible if the NDG-2.8 runs had been forced by different boundary conditions than their CTRL counterparts.

Thanks for this comment. We acknowledge that the information of this sentence is not fully explanatory. This conclusion arises from the results we obtained in the seasonal simulations of the complete autumn period. Given the large number of heavy precipitation cases during that season and the advantage of having nudged GPS data continuously, we were able to ascertain which cases were impacted the most by the GPS-ZTD nudging. Precisely we found a larger sensitivity in the model for those cases of weak synoptic forcing such as IOP16 where the role of the local factors (i.e. latent instability, low-level moisture, wind convergence and orographic triggering) is more important for convection than the direct forcing of the large scale.

To clarify this question, we include here results of the analysis on all cases of the Autumn 2012 period. These graphs will not be included in the new version of the manuscript as they would be outside the scope of the paper but will be included in a future publication from our working group. We include them here for clarification of the raised question. Finally, in the new version of the abstract this point will be adequately explained and referenced.
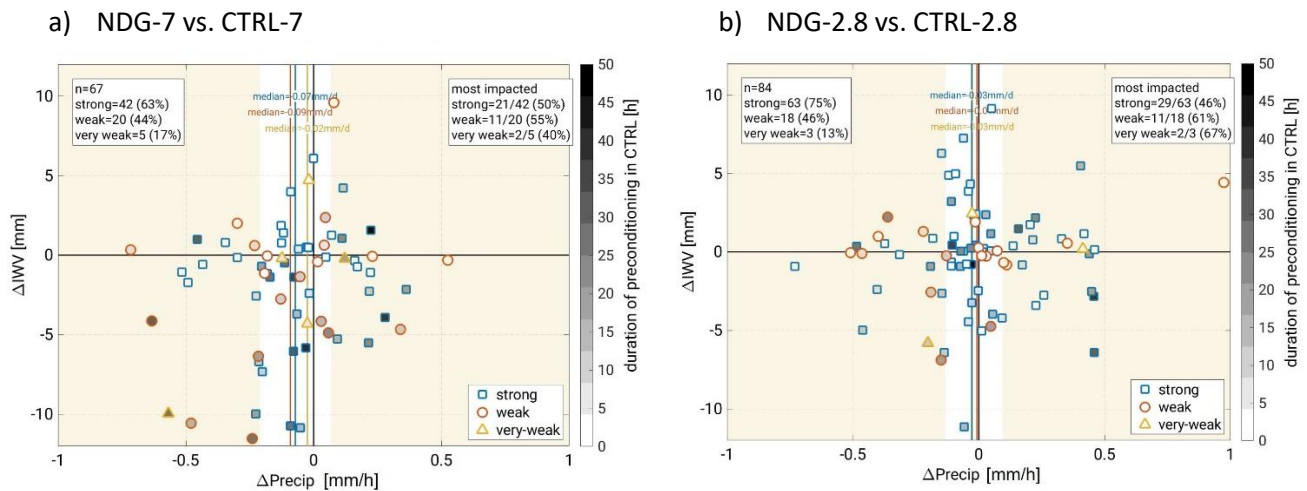
Figure 4. Scatterplot of IWV and precipitation variations due to the GPS-ZTD nudging for all events in the 1-Sep to 20-Nov period for the 7 km (a) and the 2.8 km (b). Each, dot accounts for one event. The events are detected by averaging hourly precipitation values over 8 study regions, of the HyMeX campaign (Ducrocq, 2015) and selecting those with average precipitation reaching 0.4 mm/h. The differences in precipitation and IWV (ΔPrecip, ΔIWV) are obtained after subtracting the average precipitation of NDG to CTRL. The degree of synoptic forcing (strong, weak, very weak) is calculated following the convective-adjustment time-scale criteria of Keil et al. (2013). The gray-scale color bar shows the duration of the event in the CTRL-7 and CTRL-2.8 runs respectively. The yellow shaded areas at the sides denote the areas of the upper and lower quartiles of precipitation variations. The upper-left and upper-right text boxes show statistics on the shown events.

In Fig. 4 we show the differences of IWV and precipitation for the events of the Autumn 2012 period between CTRL and their NDG counterparts (NDG-CTRL). We can see that 67 and 84 events took place in the total of the 8 investigation areas of the HyMeX campaign in the 7 km and the 2.8 km runs respectively. We can see, that 63 % of the cases in the 7 km runs and 75 % in the 2.8 km where categorized as synoptically strongly forced by the

convective adjustment time scale criteria, being the rest of them either weakly or very weakly forced. The events lying in the upper and lower quartiles of the precipitation distribution (yellow shaded areas) show that the most impacted events where those of a weak synoptic forcing (55 % in the 7 km runs and 61 % in the 2.8 km runs). The 2.8 km runs also show two out of three cases of very weak synoptic forcing within the upper and lower quartiles.

R1C10. Section 3.3: This section contains general statements, which are true, but are not new: writing that moisture is swept by a front and/or originates from the seas and oceans is true, but it would be much more interesting to know which fraction is swept and which fraction comes from evaporation

We agree with the reviewer that a quantification of the different terms of Evaporation and moisture flux over the investigation area NA and the Mediterranean would be most interesting. We have obtained the terms, described in Lamb et al. (2012) over the investigation areas NA (North Africa) and MED (Mediterranean Sea) for this purpose, see Fig. 5.a.

The calculation of these terms entails simplifications for example, of the turbulent and microphysical processes that introduce relevant uncertainties. Hence, what we provide here is an estimation of the different contributions.

$$\Delta IWV = E + (-P) + MFC \qquad\qquad\qquad\qquad\qquad\qquad\qquad\qquad (1)$$

All terms of Eq. 1 are expressed in mmh^{-1}, where positive signs of the Evaporation (E) and Integrated Moisture Flux Convergence (MFC) imply an increase of Integrated Water Vapour variations (ΔIWV>0) within the NA and MED volumes. On the contrary, if precipitation and water vapor divergence occur (MFC<0) IWV decreases (ΔIWV<0). The volumes cover the areas in Fig. 5.a where the integrations of IWV and MFC are performed from the first to the last model levels.

Fig. 5.b shows similar information to Fig.6.c of the manuscript. Intense precipitation occurs over NA on the 20-Oct-2012 with the subsequent decrease of IWV, and intense evaporation over the area on the 21-Oct and 22-Oct at midday. This is the moment when solar radiation is strongest and evaporation is intensified over this wet soil. Please note the change in the axis scales between the different panels of this figure and those of Fig.6.c of the manuscript, expressed in mmd^{-1}. The order of magnitude of those evaporations over NA is the same as those over the Mediterranean Sea, up to 0.15 mmh^{-1}. This is better seen in Fig. 5.c. The evaporated moisture is advected with the wind flow, merging with the Atlantic and Mediterranean moisture.

To quantify how much the Mediterranean Sea contributed to the changes of atmospheric moisture at that location, Fig. 5.c shows the contribution from each of the moisture equation terms over the selected volume MED. We can see that between 22-Oct and 26-Oct 1200 UTC there is a positive, homogeneous evaporation from the Sea at a rate of 0.25 mmh^{-1} that picks up from 26-Oct 1200 UTC to 0.5 mmh^{-1} by 28-Oct 0000 UTC. The time of the evaporation pick up coincides the occurrence of precipitating convection over the Mediterranean Sea west of Corsica. The intensification of the evaporation is brought by the intensified drag of horizontal winds close to sea surface.
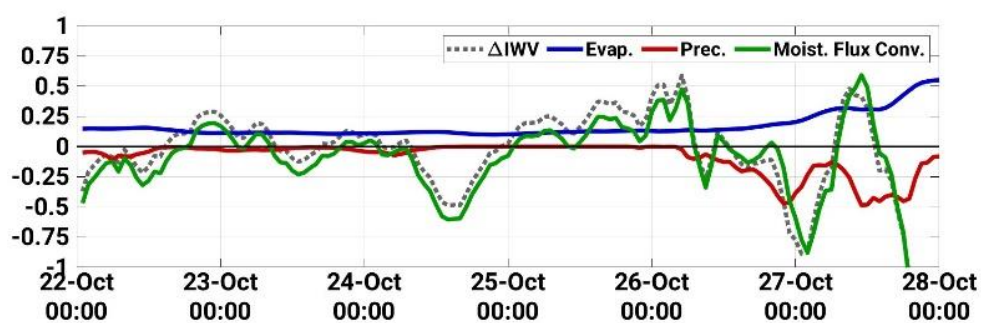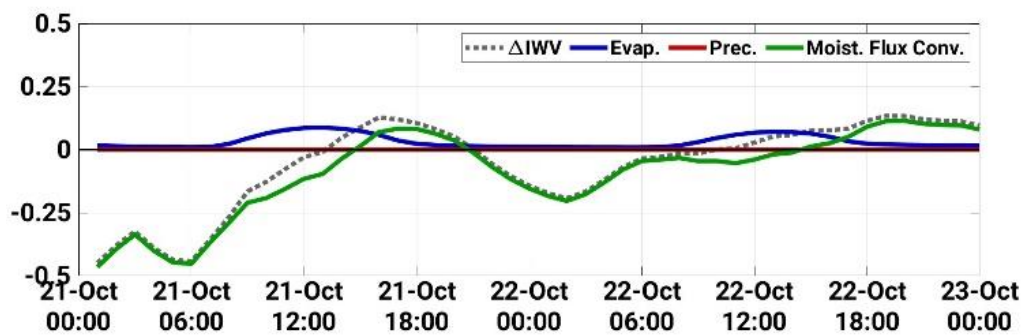
a)
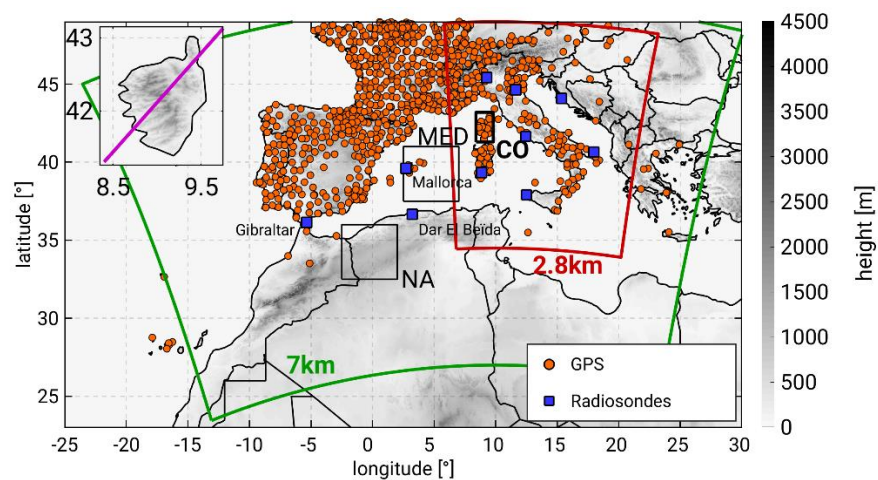
b) NA
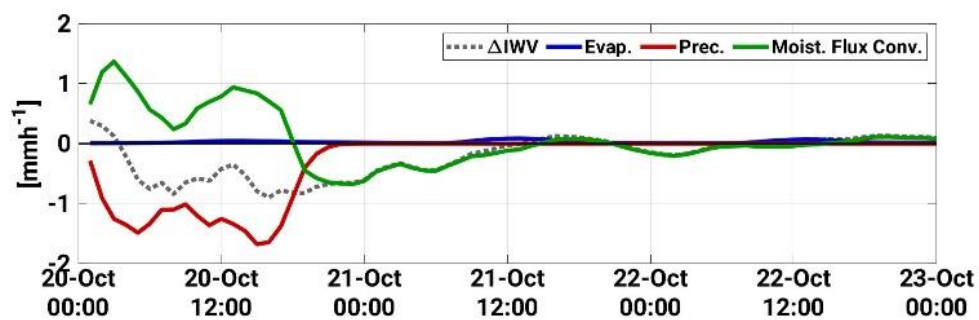
c) MED

d) NA

Figure 5. Analysis of the moisture budget terms. (a) Simulation domains as Fig.1 of the manuscript including the NA and MED areas for calculation of averaged evaporation, precipitation and moisture convergence. (b) Spatial average of hourly IWV variations (dotted grey), Evaporation (blue), Precipitation (red) and Moisture flux Convergence (green) in mmh^{-1}, over investigation area NA between 20-Oct and 23-Oct 0000 UTC. All variables are obtained from the CTRL-7 runs. (c) is as panel (b) but showing the averages over the investigation area MED between 22-Oct and 28-Oct 0000 UTC. (d) is as panel (b) but showing the spatial averages between 21-Oct and 23-Oct 0000 UTC. Mind the changes in the y-axis scaling.

R1C11. The CTRL-7 simulation is validated later (that would be better here or before!)

We will change this accordingly in the next version of the manuscript.

*R1C12. no moisture budgets are computed,*

See above

R1C13. A validation against MODIS is mentioned but not shown(?!)

We decided not to include this validation against MODIS IWV (version D3, daily product, 1°x1°, onboard Terra and Aqua) since some pixels had missing values. This is due to the inability of MODIS to retrieve IWV when there is cloud cover (Seemann, et al., 2003). Under these lines you can see the validation. Over the eastern Spanish coast and southern France on the 25-Oct-2012 and over the Alps and northern Italy on the 26-Oct-2016 there is no available MODIS data. For the areas with available MODIS data both Terra and Aqua MODIS observations overestimate IWV west of Corsica and Sardinia (25-Oct) and south of Italy (26-Oct) as compared to COSMO-CLM.

Given this issue of too many pixels showing missing values we decided not to include these figures in the manuscript and base our analysis on the model data, radiosondes and GPS.
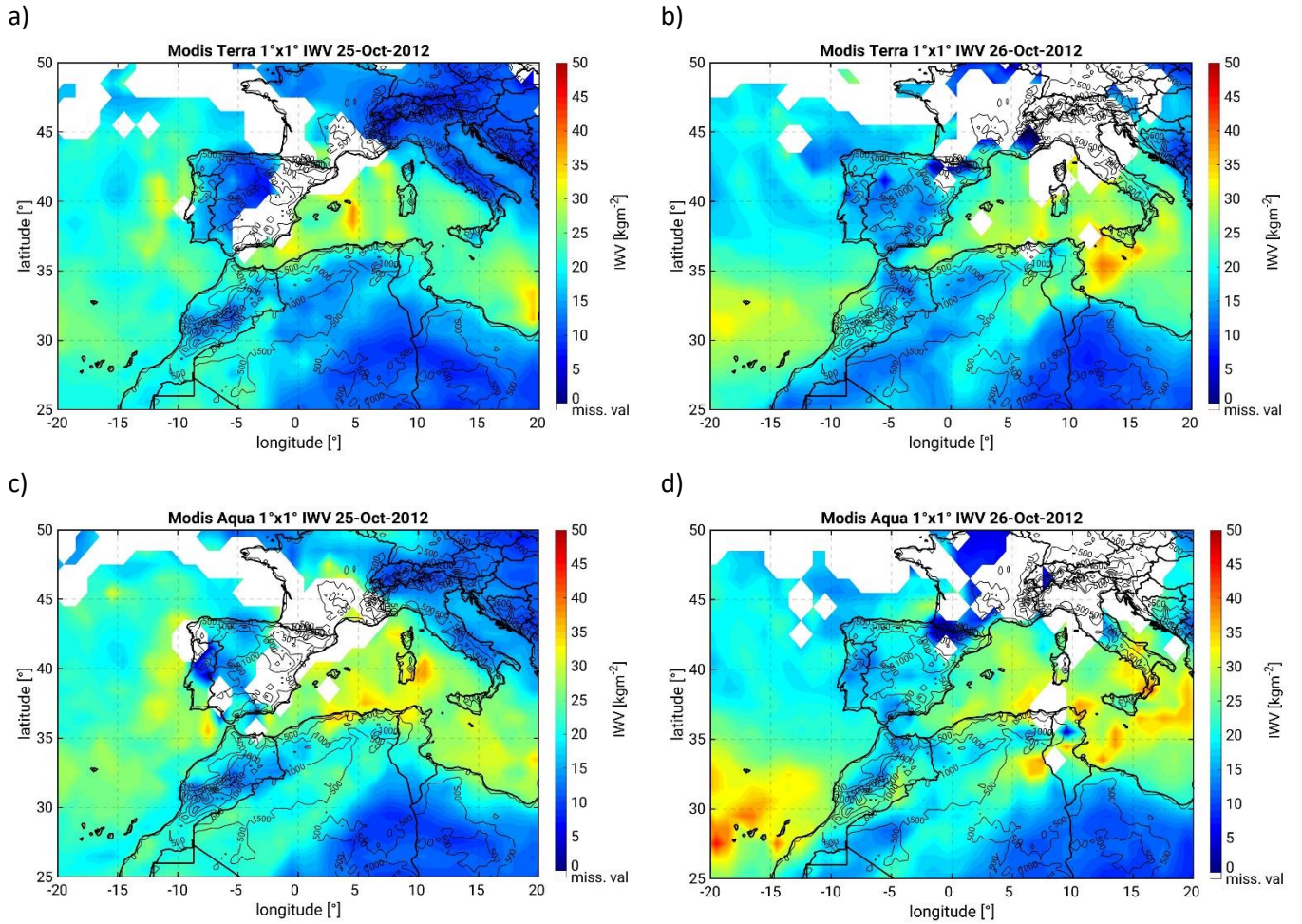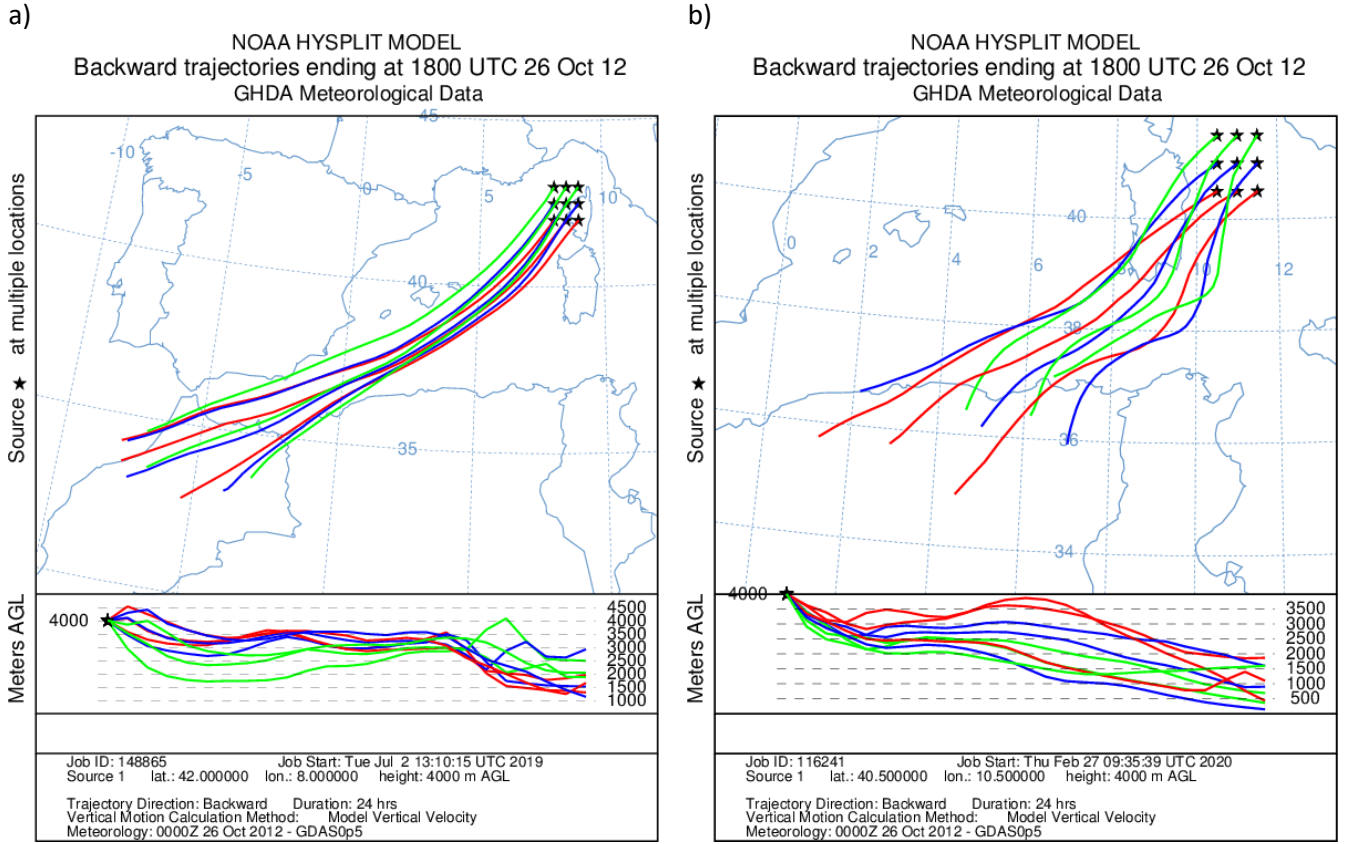
Figure 6. Daily averaged IWV measured MODIS onboard Terra (a, b) and Aqua (c, d). The spatial resolution is 1°x1°. The products used are MOD08_D3 and MYD08_D3.

R1C14. Furthermore, I suspect that labels A and B are inverted in the lower panel of Figure 6.b. If I am wrong, it means that I don't understand this panel.

The ellipses A and B try to explain which trajectories are found at which height in the GDAS-HySPLIT simulation. The fastest backward trajectories (those starting at the northwest corner of the island) are denoted with the ellipse A. On the other hand, ellipse B denotes the slower trajectories starting at the southeast corner of the matrix that reach northern Algeria in 24 h. We performed further analyses of these trajectories using the GDAS-HySPLIT model splitting the matrix of starting points. We saw that the first group of trajectories (ellipse A, reaching the Atlantic Ocean) travel for most of the 24 hours between the levels of 4000 m and 2000 m. On the other hand, the slow trajectories (ellipse B) in the last 12 h of the trajectory descend and travel at a height between 2000 m and 500 m. This is shown in the following graphs, that will be included as supplementary material in the next version of the manuscript. Moreover, a clearer explanation of the figure will be included in order to avoid the misinterpretation of this result.

a)

NOAA HYSPLIT MODEL
Backward trajectories ending at 1800 UTC 26 Oct 12
GHDA Meteorological Data

b)

NOAA HYSPLIT MODEL
Backward trajectories ending at 1800 UTC 26 Oct 12
GHDA Meteorological Data

Figure 7. Lagrangian backward trajectories obtained with the HYSPLIT model, starting on the 26-Oct-2012 1800 UTC (initiation of the event over Corsica) back to for 24 h. Figure 7.a shows the northwest subset of the trajectories shown in Fig.6.d of the manuscript while Fig. 7.b shows the subset corresponding to the trajectories starting at the southeast of the investigation domain. Please not the changes of axis (longitude, latitude and height) shown between panels a and b.

R1C15. L352-353: Why does this "further promote the moisture uptake form the Sea"?

Lifting over the affected area is accompanied by strong low-level convergence close to the surface following the mass-continuity conservation law. Stronger surface winds induce larger evaporation rates over water or wet and vegetated soils (Schneider, et al., 2010; Peixoto & Abraham H. Oort, 1992). In CCLM this process is parameterized through the standard Bulk-Transfer scheme (Louis, 1979) that controls the heat and mass transfer between the surface (land or water) and the atmosphere (Schättler, et al., 2016). In this scheme, the surface water flux affects the atmosphere as lower boundary conditions for the turbulent moisture flux ($F_{q^v}^3$) within the turbulent mixing term of the model equations ($M_{q^v}^{TD}$). The turbulent moisture flux ($F_{q^v}^3$) is proportional to the horizontal wind speed over the surface ($|\overrightarrow{v_h}|$) following the next equation.

$$\left(F_{q^v}^3\right)_{sfc} = -\rho C_q^d |\overrightarrow{v_h}|\left(q^v - q_{sfc}^v\right) \tag{1}$$

Where ρ is the air density, C_q^d is the bulk-aerodynamical coefficient for turbulent moisture transfer, which is adapted to each surface type (water, soil type, vegetation, etc), q_{sfc}^v is the ground specific humidity and q^v is the humidity at the lowest model level. Hence, larger moisture flux from the surface (land, sea) to the atmosphere happens with larger horizontal wind speeds.

R1C16. L396-398: Looking only at the maximum precipitation value is not really fair because the RG network is rather sparse compared to the scale of the studied phenomenon (and simulated maximum value). At first glance,

I would say that CTRL-2.8 is better than NDG-2.8. A proper validation of numerical simulations against RG is needed.

We decided to validate our model results against the HyMEX RG data set given it has undergone several post-processing procedures (four revised versions of the product, https://mistrals.sedoo.fr/?editDatsId=904&datsId=904&project_name=HyMeX) and enjoys a large quality. We performed another validation against the CMORPH product, which has a spatial scale (8 km), similar to the model resolutions (7 km and 2.8 km) but found large discrepancies between CMORPH and RG for this case study. Therefore, we dismissed the analysis against CMORPH.

We acknowledge that a point-to-point comparison against RG entails difficulties, such as the sparse distribution over the island, as pointed out by the reviewer, and the double-penalty problem due to missed location of precipitation maxima (Wernli, et al., 2008; Gilleland, et al., 2009). This is why, in the comparison against RG (Tables 1 and 3) we perform a point-to-point comparison interpolating to the location of the stations but also analyse the maximum and standard deviation of the precipitation distributions intensities over the island. Since RG are usually employed as reference data for precipitation validation (Habib, et al., 2012; Jiang, et al., 2018) we decided to use this data set for the validation.

We show here the validation metrics similarly to Table 1 for the seasonal simulations (initialized on 01-Sep-2012). For the calculation of the metrics, hourly and accumulated precipitation values between 26-Oct 1300 UTC and 27-Oct 1700 UTC i.e. the period of precipitation over CO.

We confirm the comment of the reviewer for the 2.8 km since CTRL-2.8 outperforms NDG-2.8 in the simulation of the standard deviations of precipitation (both hourly and accumulated), accumulated precipitation and maximum. Only, the hourly RMSE is improved in NDG-2.8.

Regarding the 7 km simulations, applying the GPS-ZTD nudging is beneficial in that it improves the RMSE, and the standard deviation and maximum value of the accumulated precipitation values. This is as described in the manuscript.

These results can be explained from the precipitation reduction of the NDG-7 and NDG-2.8 simulations. CTRL-7 was overestimating excessively precipitation, whereas CTRL-2.8 showed a good representation of the maximum and accumulated amount. After a drying, only the scores of the 7 km resolution were improved, but not those of the 2.8 km.

We will adapt our conclusions and analysis in the manuscript to suit these findings. Besides, we will include Table 3 in Section 4.1 of the manuscript.

Table 3. As, Table 1 for the runs initialized on the 1-Sep-2012. The validation is done against hourly or accumulated precipitation values between 26-Oct 1300 UTC and 27-Oct 1500 UTC i.e. the period of precipitation over CO.

	Interp. To RG location			Distributions without interpolation	
	RMSE (1h)	$OBS_\sigma - MOD_\sigma$ (1h)	$\overline{OBS} - \overline{MOD}$ (27h)	$OBS_\sigma - MOD_\sigma$ (27h)	$OBS_{max} - MOD_{max}$ (27h)
CTRL-7-Init1Sep	3.1	-0.35	-10.4	-56	-185
NDG-7- Init1Sep	2.6	1.07	15.4	-0.7	-58
CTRL-2.8-Init1Sep	3.1	0.55	14.6	6	-3
NDG-2.8-Init1Sep	2.7	1.03	21.5	12	11

Only two sets of simulations can be validated against radiosondes. On the one hand, the free runs (CTRL), where no observation nudging is performed and hence are runs constrained only by the forcing data. On the other hand, the NDG runs where IWV is corrected every 10 minutes. We are assessing the accuracy of model moisture output for these two different sets of simulations.

Regarding the comment on the proximity between the GPS stations and the radiosondes. We must add that CCLM redistributes the nudged GPS information in the vertical profile specific humidity. Hence CCLM constructs a profile where errors at some levels are introduced. This is exactly what we wanted to quantify in Section 4.2 and Figures 8 and 9.

Yes, thanks for this remark. Indeed, the spatial averages shown in Fig.8.a are obtained from the area CO and not Corsica. The text has been changed accordingly in the manuscript. In now reads:

Figure 8.a shows the spatially averaged temporal evolution of IWV over CO. The hours prior to precipitation initiation (26-Oct 1300 UTC) were characterized by an IWV pick up starting at 26-Oct 0000 UTC. All simulations show this, albeit the IWV amount over CO for NDG-7 and NDG-2.8 was 5 mm higher than for CTRL-7 and CTRL-2.8. This was due to represented precipitation over the island until the night of 24-Oct in the NDG runs, hence inducing a much wetter boundary layer (not shown).

How the GPS-ZTD nudging affects the vertical distribution of humidity is introduced in Section 4.2, in Figs. 8.b and Fig. 9. This is done on the one hand through box and whiskers plots over the investigation domain CO (Fig. 8.b) and on the other hand in the validation of the CCLM atmospheric moisture distribution against radiosondes (Fig 9). The sentence, as pointed out by the reviewer, could be misleading since no reference to the figures is given. We have corrected this in the manuscript. Furthermore, Fig. 8 shows how between 26-Oct-2012 1300 UTC and 27-Oct-2012 1500 UTC the specific humidity median, quartile and extreme values at 500 hPa are lower in NDG as compared to CTRL. We will revise our manuscript to read "*The humidity reduction between 26-Oct 1600 UTC and 27-Oct 0600 UTC takes mostly place at 500 hPa down to the 950 hPa level*".

The validation against radiosondes of Section 4.2 had for objective showing how good was the performance of the model in representing the profile of specific humidity. We selected all operational stations available during the two days of convective activity in the Mediterranean contained within the simulation domains of both resolutions. Hence the seven stations shown in Fig. 1 of the manuscript. Even if the stations are located only east of the study region on the Italian Peninsula, they are still valuable to assess the performance of the model.

Thanks for this remark. In the analysis of box and whisker plots for 2m specific humidity we saw a reduction of ca. 1 gkg^{-1} and 0.5 gkg^{-1} in the NDG-7 and NDG-2.8 respectively as compared to their CTRL counterparts. This was shown for the period between 26Oct 1300 UTC and 27-Oct 1500 UTC over Corsica. We did not include this graph in our manuscript in order to make the text more concise, but we will include it as a subpanel of Fig. 8.b in the next version of our manuscript. Figure 8.b then will show as it follows
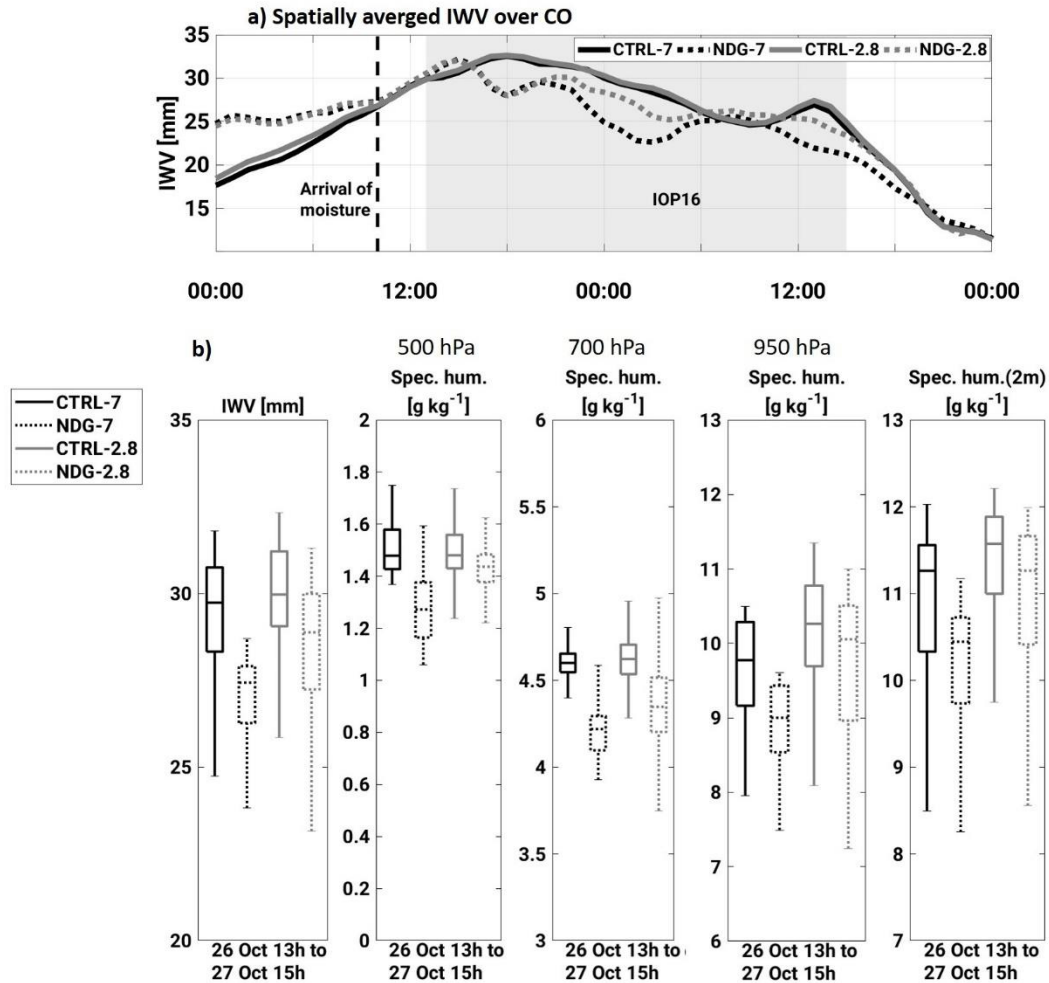

Figure 8. Spatially averaged IWV for all simulations during the event. The area for averaging is shown in Fig. 1 (CO) and the model output has been upscaled to a common coarser grid. The period shown is 26-Oct 0000 UTC to 28-Oct 0000 UTC. (b) Box and whiskers plots showing the median, the percentiles 25 and 75 and the extreme values of IWV and specific humidity at 500 hPa, 700 hPa,950 hPa and at 2m height. All box and whiskers are obtained from the distribution of values for the shown quantities between the 26-Oct 1300 UTC and 27-Oct 1500 UTC over the study region CO.

R1C22. L469-471: A simulation nudging IWV at 2.8 km and forced by NDG-7 would be useful here.

As explained in Section 1, we decided to force the NDG-2.8 runs with CTRL-7 to allow for comparison against CTRL-2.8. We believe this is the best means to assess the direct impact of the GPS-ZTD nudging in this resolution, avoiding any potential influences coming from the forcing data.

R1C23. L487: Why is the effect of the low-pressure system change exclusively seen in the 7 km simulations? Isn't the wind changed in the 2.8 km simulations, too?

We show only the results in the 7 km resolution since these runs cover the whole western Mediterranean area, as opposite to the 2.8 km runs. The 2.8 km simulation domain only covers the Italian Peninsula and the islands in order to save computational resources. The effect described in the manuscript (increase of PMSL at the centre of the low-pressure system in southern France) is only seen in the NDG-7 simulation since NDG-2.8 does not cover southern France. The following figure shows the PMSL changes in the NDG-2.8 compared to CTRL-2.8 and in the winds at 950 hPa (analogously to Fig. 12 in the manuscript for the 7 km runs).
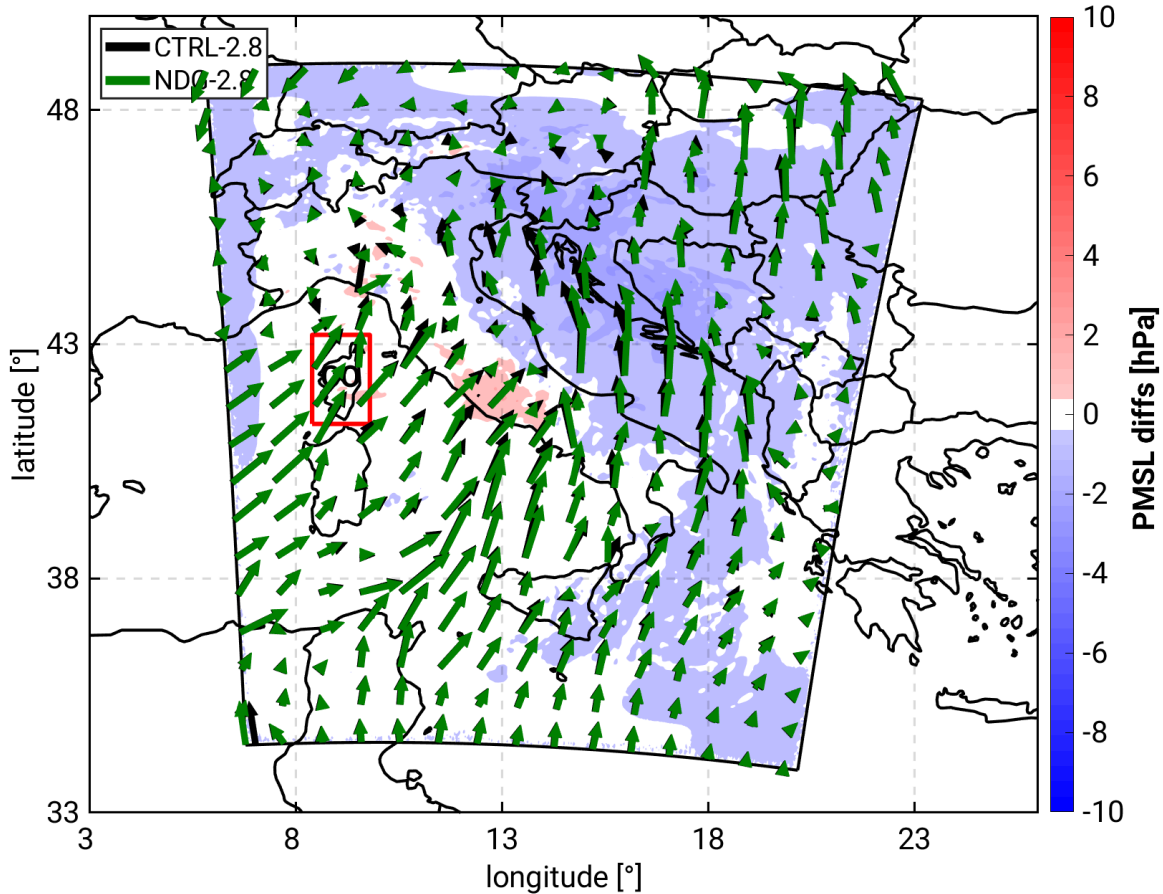
Figure 9. Spatial distribution of the differences in Pressure at the Mean Sea Level (PMSL) between NDG-2.8 and CTRL-2.8 on the 26-Oct 2300 UTC. Horizontal winds at 950 hPa are represented by black (CTRL-2.8) and green (NDG-2.8) arrows.

Fig. 9 shows that there are some areas (Adriatic Sea, the Balkans, southern Alps) with lower PMSL in the NDG-2.8 than CTRL-2.8 in extent of -2 hPa. These differences are weaker than the differences observed in the 7 km runs (up to 10 hPa) and are of opposite sign. Fig.9 clearly shows that the NDG-2.8 run does not show the same effect as NDG-7. The weakening of the low-pressure system over southern is not simulated in the NDG-2.8. There are however changes in the wind direction and intensity, mainly offshore, ahead of the western Italian and the Balkan coasts. However, these changes in wind direction and speed do not correspond to the changes observed in the 7 km runs since they do not show a clockwise veering of the direction centered in the southern French region. We will also include this graph in the supplementary material to support the analysis of the PMSL variations in Section 4.4

In the general comments part, we have addressed how only little differences arise from using different nudging frequencies for spatially averaged precipitation in the 7 km for this case study over CO. These findings will be presented in the new version of the manuscript in Section 4.1 (Nudging effects on Precipitation).

3-TECHNICAL CORRECTIONS

We have accepted all corrections and comments of this section in the revised version of the manuscript. Where needed a short clarification is added here.

We have adapted these lines in the manuscript to give this information in a clearer way. How the information is spread in the vertical direction is relevant since each GPS observation is used to construct a specific humidity profile that is treated as such in the nudging scheme. Hence, what is used for the nudging is this constructed profile based on the issued GPS-ZTD value. This sentence has been rewritten as: *"The vertical interpolation of the observed data is performed assuming a Gaussian decay in height differences. The vertical interpolation is also applied in the case of GPS-ZTD nudging since a profile of specific humidity is constructed from the derived GPS-IWV value. This constructed profile shall be treated by the nudging scheme as an upper-air measurement in the remainder of the process."*

Yes, it is an iterative process that its repeated until a sufficiently low error is reached or after 20 iterations. We acknowledge that Eq. (2) in the manuscript was not written as an iterative formula and we have corrected this. This paragraph now reads.

"The observations are assigned to a grid point in the model space, provided the altitude difference of the GPS station and model surface lays within the range -150 to 600 m to allow for extrapolation and interpolation, respectively and are converted to a specific humidity profile (q_v^{mod}). This is needed given IWV is not a model prognostic variable as opposite to specific humidity. The profile is constructed by means of an iterative process that scales the observed IWV (IWV^{obs}) with the modelled one (IWV^{mod}) until a sufficiently low error is reached or up to 20 iterations. Eq. (2) describes the iterative formula. The first profile ($q_{v_i}^{mod}$) used as the first guess for the iterative process, is the modelled specific humidity profile. Hence, the profile used for nudging depends on the vertical humidity distribution simulated by the model at the beginning of the nudging time-window. "

$$q_{v_{i+1}}^{mod} = q_{v_i}^{mod} \cdot \frac{IWV^{obs}}{IWV_i^{mod}} \tag{2}$$

Every 6 h. The forcing data has a temporal resolution of 6 h. We have included this information in the newest version of the manuscript.

This sentence has been rephrased to express the information in a clearer way. In it, we were referring to a large reduction of maximum precipitation that was induced by the GPS-ZTD nudging. We have added more details so that this sentence is not out of context. The sentence now reads.

"Within the 80-day period of simulation, there were several events, which were largely affected by the GPS-ZTD nudging. IOP16, the case study of this paper, is one of them which is especially interesting given the large reduction of maximum precipitation (-20 %) induced by the GPS-ZTD nudging over the investigation area of Corsica in the course of 26 h. IOP16 is also suitable to assess the benefit of atmospheric moisture corrections with GPS-ZTD nudging given the important role of the local orographic and instability factors in triggering and maintaining convection rather than the large-scale upper level forcing."

R1C29. L298: What is an "offshore-size" convective system?

Thy is a typo. The sentence should read "Between 26-Oct 1900 UTC and 27-Oct 0100 UTC, offshore convective systems arrive at the island (see Fig.3.a)". We have corrected the text accordingly.

R1C30. L447: What is an "accuracy rate"?

The corrected sentence is: "The 2.8 km simulation was initially more accurate, but the nudging brings both to similar accuracy values".

R1C31. L454: What does "height-surface" mean? Do the authors simply mean "vertical"?

Yes, it was meant vertical cross-section. Thank you. It has been corrected in the manuscript.

R1C32. L455: What does "vertical-horizontal direction" mean?

The sentence has been changed to: "Figure 10 shows the vertical cross-sections of Equivalent Potential Temperature (θ_e), specific humidity and the wind along the direction of the mean horizontal wind (purple transect in Fig. 1) over the island at 26-Oct 1700 UTC."

4-REFERENCES

Benjamin, S. G. et al., 2010. Relative Short-Range Forecast Impact from Aircraft, Profiler, Radiosonde, VAD, GPS-PW, METAR, and Mesonet Observations via the RUC Hourly Assimilation Cycle. *Monthly Weather Review,* 4, Band 138, p. 1319–1343.

Borderies, M. et al., 2019. Assimilation of wind data from airborne Doppler cloud-profiling radar in a kilometre-scale NWP system. *Natural Hazards and Earth System Sciences,* 4, Band 19, p. 821–835.

Gilleland, E. et al., 2009. Intercomparison of Spatial Forecast Verification Methods. *Weather and Forecasting,* 10, Band 24, p. 1416–1430.

Habib, E., Haile, A. T., Tian, Y. & Joyce, R. J., 2012. Evaluation of the High-Resolution CMORPH Satellite Rainfall Product Using Dense Rain Gauge Observations and Radar-Based Estimates. *Journal of Hydrometeorology,* 12, Band 13, p. 1784–1798.

Jiang, Q. et al., 2018. Accuracy Evaluation of Two High-Resolution Satellite-Based Rainfall Products: TRMM 3B42V7 and CMORPH in Shanghai. *Water,* 1, Band 10, p. 40.

Keil, C., Heinlein, F. & Craig, G. C., 2013. The convective adjustment time-scale as indicator of predictability of convective precipitation. *Quarterly Journal of the Royal Meteorological Society,* 5, Band 140, p. 480–490.

Lamb, P. J., Portis, D. H. & Zangvil, A., 2012. Investigation of Large-Scale Atmospheric Moisture Budget and Land Surface Interactions over U.S. Southern Great Plains including for CLASIC (June 2007). *Journal of Hydrometeorology,* 12, Band 13, p. 1719–1738.

Louis, J.-F., 1979. A parametric model of vertical eddy fluxes in the atmosphere. *Boundary-Layer Meteorology,* Band 17, pp. 187-202.

Mahfouf, J.-F., Ahmed, F., Moll, P. & Teferle, F. N., 2015. Assimilation of zenith total delays in the AROME France convective scale model: a recent assessment. *Tellus A: Dynamic Meteorology and Oceanography,* 2, Band 67, p. 26106.

Peixoto, J. P. & Abraham H. Oort, 1992. *Physics of Climate.* s.l.:American Inst. of Physics.

Sahlaoui, Z., Mordane, S., Wattrelot, E. & Mahfouf, J.-F., 2019. Improving heavy rainfall forecasts by assimilating surface precipitation in the convective scale model AROME: A case study of the Mediterranean event of November 4, 2017. *Meteorological Applications,* 12.Band 27.

Schättler, U., Doms, G. & Schraff, C., 2016. *A Description of the Nonhydrostatic Regional COSMO-Model Part VII : User's Guide,* DeutscherWetterdienst, P.O. Box 100465, 63004 Offenbach, Germany: s.n.

Schneider, M. et al., 2010. Continuous quality assessment of atmospheric water vapour measurement techniques: FTIR, Cimel, MFRSR, GPS, and Vaisala RS92. *Atmospheric Measurement Techniques,* 3, Band 3, p. 323–338.

Seemann, S. W., Li, J., Menzel, W. P. & Gumley, L. E., 2003. Operational Retrieval of Atmospheric Temperature, Moisture, and Ozone from MODIS Infrared Radiances. *Journal of Applied Meteorology,* 8, Band 42, p. 1072–1091.

Wernli, H., Paulat, M., Hagen, M. & Frei, C., 2008. SAL—A Novel Quality Measure for the Verification of Quantitative Precipitation Forecasts. *Monthly Weather Review,* 11, Band 136, p. 4470–4487.